An Investigation into the Influence of Electrospinning Parameters on the Diameter and Alignment of Poly(hydroxybutyrate-*co*-hydroxyvalerate) Fibers

Ho-Wang Tong, Min Wang

Department of Mechanical Engineering, The University of Hong Kong, Pokfulam Road, Hong Kong, People's Republic of China

Received 13 May 2010; accepted 28 August 2010
DOI 10.1002/app.33302
Published online 1 December 2010 in Wiley Online Library (wileyonlinelibrary.com).

ABSTRACT: Electrospinning is an effective technology for the fabrication of ultrafine fibers, which can be the basic component of a tissue engineering scaffold. In tissue engineering, because cells seeded on fibrous scaffolds with varying fiber diameters and morphologies exhibit different responses, it is critical to control these characteristics of electrospun fibers. The diameter and morphology of electrospun fibers can be influenced by many processing parameters (e.g., electrospinning voltage, needle inner diameter, solution feeding rate, rotational speed of the fiber-collecting cylinder, and working distance) and solution properties (polymer solution concentration and conductivity). In this study, a factorial design approach was used to systematically investigate the degree of influence of each of these parameters on fiber diameter, degree of fiber alignment, and their possible synergetic effects, using a natural biodegradable polymer, poly(hydroxybutyrate-*co*-hydroxyvalerate), for the electrospinning experiments. It was found that the solution concentration invoked the highest main effect on fiber diameter, whereas both rotational speed of the fiber-collecting cylinder and addition of a conductivity-enhancing salt could significantly affect the degree of fiber alignment. By carefully controlling the electrospinning parameters and solution properties, fibrous scaffolds of desired characteristics could be made to meet the requirements of different tissue engineering applications. © 2010 Wiley Periodicals, Inc. J Appl Polym Sci 120: 1694–1706, 2011

Key words: electrospinning; biofibers; biodegradable; biomimetic; tissue engineering scaffold

INTRODUCTION

Electrospinning is an effective and versatile technology for fabricating ultrafine fibers, which can be used to construct tissue engineering scaffolds that assist in regenerating different types of human tissues such as bone, cartilage, tendon, ligament, skin, nerve, and blood vessel.[1–5] Depending on the specific tissue engineering applications, fibers of different diameters are usually required. Because most biological tissues consist of nanoscaled collagen fibers or fibrils, nanofibers are usually preferred to construct tissue engineering scaffolds to mimic the extracellular matrix of various biological tissues.[6] It was also reported that nanofibrous scaffolds can exhibit actual benefits toward tissue engineering applications because of their large surface areas to adsorb proteins that provide binding sites to cell membrane receptors.[7] On the other hand, some nanoparticles such as hydroxyapatite can be incorporated into the electrospun fibers to enhance the osteoconductivity of the fibers for bone tissue engineering applications.[8–10] In this case, microfibers are preferred because it is easier for microfibers to encapsulate nanoparticles than for nanofibers. This shows the importance of considering the fiber diameter when different types of tissue engineering scaffolds are constructed. More importantly, the fiber diameter of a fibrous scaffold is one of the most important biomaterial design features that can influence the response of cells and formation of tissues. Sanders et al.[11] assessed the effect of fiber diameter on the fibrous tissue capsule thickness for electrospun fibers in subcutaneous dorsum tissue. They found that the geometric feature of microfiber diameter played a critical role in affecting the formation of fibrous capsule. Chen et al.[12] investigated the effect of fiber diameter on adhesion and proliferation of NIH 3T3 fibroblast on electrospun fibrous scaffolds, and they claimed that cell adhesion and growth kinetics increased with decreasing fiber diameter. Badami et al.[13] also demonstrated the significant effect of fiber diameter on spreading, proliferation, and differentiation of osteoblastic cells on electrospun fibers, whereas Moroni et al.[14] reported the fiber diameter effects on cell attachment, proliferation, and spreading. Therefore, the effect of various

Correspondence to: M. Wang (memwang@hku.hk).
Contract grant sponsor: The University of Hong Kong (HKU).
Contract grant sponsor: Research Grants Council of Hong Kong; contract grant number: GRF grant HKU 7176/08E.

TABLE I
Determination of Electrospinning Parameters for the Factorial Design Experiments

Electrospinning parameter	Role of the parameter in influencing electrospun fiber diameter and morphology
Concentration of PHBV solution	Polymer solution concentration affects the solvent evaporation duration during electrospinning, which, in turn, affects the stretching duration of the polymer jet and hence the final fiber diameter and morphology
Electrospinning voltage	Electrospinning voltage affects the electric force that stretches the polymer jet into ultrafine fiber and hence affects the fiber diameter and morphology
Needle inner diameter	Needle inner diameter affects the size of Taylor cone and hence the diameter of initial jet from the cone and the resulting fiber diameter
Solution feeding rate	Solution feeding rate affects the volume of polymer solution supplied to the Taylor cone from which the polymer jet is initiated
Concentration of BTEAC	Concentration of BTEAC affects conductivity of polymer jet, which, in turn, influences the electric stretching force exerted on the jet
Rotational speed of fiber collector	Rotational speed of fiber collector affects the degree of fiber stretching and fiber orientation when the fiber lands on the collector
Working distance	Working distance affects the trajectory of polymer jet and hence the traveling distance of the jet, which, in turn, affects the stretching duration of the jet

electrospinning parameters on electrospun fiber diameter has attracted considerable attention.[15–27]

Fiber alignment is another important characteristic that can influence cell response and tissue formation and, hence, determine the performance of fibrous scaffolds in some tissue engineering applications. Chew et al.[28] investigated the effect of the fiber alignment for electrospun fibrous scaffolds and found that Schwann cell maturation preferentially occurred on aligned fibers rather than randomly oriented fibers. Mills et al.[29] reported that MG63 cells tended to align with the pattern of structures for cell seeding. Xu et al.[30] and Yang et al.[31] demonstrated the advantages of using aligned fibers in blood vessel engineering and neural tissue engineering, respectively. It is also worth noting that aligned fibers should be very useful for the tissue engineering of tissues such as tendon and ligaments because of the similarity between the aligned topography of the fibers in the electrospun scaffolds and the aligned topography of the fibers in the natural extracellular matrix of these types of tissues.

Although the effects of electrospinning parameters on fiber alignment were not often investigated, the parameter effects on fiber diameter have been regularly reported. In most of these investigations, researchers used the one-factor-at-a-time method of experimentation, in which electrospinning parameters were varied one at a time, with the remaining parameters being kept unchanged. Using the one-factor-at-a-time method, the effects of polymer solution concentration,[15,16] electrospinning voltage,[19–21] needle inner diameter,[22] working distance,[23] and solution flow rate[25,26] on fiber diameter were investigated. However, the one-factor-at-a-time method can only provide an estimation of the effect of a single parameter at selected and fixed conditions of the other parameters. To claim the validity of such estimation, it is essential to assume that the effect is the same at all the other settings of the remaining parameters, which may not be true. To prove or disprove this assumption, a researcher needs to perform the one-factor-at-a-time experiments at every possible combination of parameters. However, conducting experiments in this way is tedious and time-consuming because many experimental runs are required. Also, researchers may not be able to determine which parameter has a higher degree of influence by using the one-factor-at-a-time method, even though they can assess the effect of each parameter on a certain feature. To overcome these limitations, the factorial design[32] was used to investigate the electrospinning parameters in this research. Our previous studies found that the diameter and morphology of the electrospun fibers were usually influenced by the parameters, including (A) polymer solution concentration, (B) electrospinning voltage, (C) needle inner diameter, (D) solution feeding rate, (E) concentration of conductivity-enhancing salts, (F) rotational speed of the fiber-collecting cylinder, and (G) working distance (i.e., distance between the needle and the fiber collector). The roles of these parameters in influencing electrospun fiber diameter and morphology are summarized in Table I. However, each of these parameters can have different degrees of influence on fiber diameter and morphology. To assess whether one parameter plays a more important role than the others or whether the parameters have interaction effects, these parameters could be systematically investigated through the factorial design experiments. The effects of each parameter on fiber morphologies (including fiber diameter and degree of fiber alignment) and their statistical significances could then be quantified and compared. Understanding which parameters are most influential on fiber morphologies is important for scaffold design and fabrication. The results should be very useful for the electrospinning of tissue engineering scaffolds.

The material used in this electrospinning study was poly(hydroxybutyrate-*co*-hydroxyvalerate) (PHBV), which is a copolymer of polyhydroxybutyrate (PHB) and polyhydroxyvalerate. PHB has been electrospun into ultrafine fibers, and the effects of various electrospinning parameters such as applied voltage and solution flow rate on fiber morphology were investigated. It was found that the solution flow rate played a major role in determining the electrospun PHB fiber diameter.[33] Being a natural, biocompatible, and biodegradable polymer, PHBV has also received great attention, especially in the biomedical field. Kwon et al.[34] produced PHBV nanofibers by electrospinning, and subsequent cell culture experiments demonstrated reliable cell attachment and growth on electrospun PHBV nanofibrous mat, suggesting the suitability of electrospun PHBV fibers for biomedical applications. Meng et al.[35] further improved the performance of electrospun PHBV nanofibrous scaffolds by blending PHBV with collagen, and enhanced cell adhesion and growth were reported. Different from most electrospinning studies that focused on the formation of nonwoven fibers, Chan et al.[36] fabricated aligned PHBV fibers by using a counter electrode collector or a rotating disk collector during electrospinning and found that the degree of fiber alignment improved by increasing the fiber take-up velocity. These studies have demonstrated some parameter effects on PHBV fiber morphology and the potential of PHBV fibers for biomedical applications. A deeper understanding on the effects of multiple parameters on electrospun PHBV fiber diameter and alignment is thus required for constructing fibrous PHBV tissue engineering scaffolds of desired characteristics. Therefore, the factorial design approach was applied to investigate the influences and interactions of electrospinning parameters for PHBV. The factorial design approach used in this study not only shed light on the formation of PHBV fibers but also contributed to the electrospinning of different polymeric fibers when this approach is adopted to study electrospinning of other polymers.

EXPERIMENTAL

Materials

The polymer used in this study was PHBV with a molecular weight of 310,000 and containing 2.9 mol % of 3-hydroxyvalerate (Tianan Biologic Material, China). The polymer was dissolved in chloroform of analytical grade (VWR BDH Prolabo, UK) at different concentrations through gentle heating and stirring by a hotplate magnetic stirrer (RET control visc IKAMA®, USA). A conductivity-enhancing salt, benzyl triethylammonium chloride (BTEAC) (Fluka, Germany), was used in this study.

Electrospinning of PHBV fibers

During electrospinning, the polymer solution was loaded into a syringe, and the solution was pushed from the syringe to a blunt-ended injection needle at a controlled feeding rate by a syringe pump (Model A99, Razel, USA). Application of a high voltage by a power supply (Gamma High Voltage Research, USA) to the needle resulted in the formation of a jet from a solution pendent droplet suspended at the needle tip. As the solvent evaporated, the jet solidified into an ultrafine fiber, which was collected by a high-speed rotating cylinder. The fiber-collecting cylinder, which was designed in-house, had been successfully used to fabricate highly aligned fibers and multilayered fibrous structures during electrospinning.[6] The electrospinning process continued, and a fibrous membrane could be obtained on the surface of the cylinder eventually.

Characterizations of electrospun fibers

The electrospun fibers were characterized using a scanning electron microscope (Stereoscan 440, UK). The fiber diameter and degree of fiber alignment were measured by analyzing the scanning electron microscopy (SEM) micrographs with an image tool (UTHSCSA). The diameters of 50 fibers were measured for each SEM micrograph, and the average fiber diameter was then calculated. The degree of fiber alignment was investigated by measuring the angle between an electrospun fiber and the longitudinal axis of the rotating cylinder. Fifty angles were measured for each SEM micrograph, and the number of fibers that aligned within specific ranges of angles was counted. In this study, the fibers that aligned between 80° and 100° relative to the longitudinal axis of the rotating cylinder were defined as highly aligned fibers.

Assessing the effects of electrospinning parameters on fiber diameter and alignment using the factorial design method

Each of the seven parameters mentioned in the introduction of this article was studied at two levels, as shown in Table II. The boundary values of each of the seven parameters were chosen such that uniform fibers without beads or polymer blocks could be obtained at a desirable fiber production rate. The problems of using parameters beyond the boundary values are also summarized in Table II (Tong and Wang, unpublished). Through the 2^{7-4}_{III} fractional factorial design, the fiber diameter and the degree of fiber alignment were determined under various combinations of conditions, as shown in Tables III and IV, respectively. The capital letters (A–G) in these tables represent the parameters being investigated, whereas the corresponding small letters

TABLE II
Boundary Values for the Seven Electrospinning Parameters Assessed and Major Defects/Problems Encountered for Using Electrospinning Parameters Beyond the Boundary Values

Code	Electrospinning parameter	Boundary values for experiments		Major defects/problems encountered for using electrospinning parameters beyond the boundary values	
		−	+	Beyond the low boundary	Beyond the high boundary
A	Concentration of PHBV (wt %)	10	15	Formation of beaded fibers/no fiber formation	Blockage of needle
B	Electrospinning voltage (kV)	15	25	Formation of polymer blocks/no fiber formation	Insufficient fibers
C	Needle inner diameter (mm)	0.5	0.8	Very low fiber production rate	Blockage of needle
D	Solution feeding rate (mL/h)	3	7	Very low fiber production rate	Risk of damaging the pump
E	Concentration of BTEAC (wt %)	0	3	No effect	Very unstable polymer jet
F	Rotational speed of fiber collector (rpm)	4,000	15,000	No effect	Breakage of fibers
G	Working distance (cm)	5	10	Formation of polymer blocks	No fiber formation

represent the dummy factors. Each string of small letters indicates an interaction of the all or two of the dummy factors a, b, and c. Two fibrous membranes were fabricated for each combination of parameters. The main effects of each parameter on fiber diameter and fiber alignment were then calculated. To distinguish between the confounding patterns, the parameters showing significant effects were subjected to the 2^3 factorial design for further analysis. The final effects were quantitatively established, whereas the statistical significance and the underlying reasons were discussed.

RESULTS AND DISCUSSION

Fiber diameter and degree of fiber alignment

Depending on different processing parameters and polymer solution properties, electrospinning could be used to fabricate PHBV fibers with different diameters and orientations. Figure 1 shows the electrospun fibers with diameters of over 1 μm (Exp. No. 5), whereas Figure 2 shows the fibers with diameters of a few hundred nanometers (Exp. No. 1). These fibers were randomly oriented without alignment. Figure 3 shows the morphology of aligned fibers obtained by electrospinning (Exp. No. 2). The degree of fiber alignment in Figure 3 is depicted by the histogram in Figure 4, which shows that more than 90% of the fibers aligned between 80° and 100° relative to the longitudinal axis of the rotating cylinder.

Estimation of the main effects

Using the results from Tables III and IV, the main effects of each of the seven parameters on fiber diameter and fiber alignment were determined. As an example, the main effect of PHBV concentration on fiber diameter was estimated as follows. Consider the results of Exp. No. 1 and Exp. No. 2 listed in Table III first. Assume that the parameters D, E, and G did not significantly affect the fiber diameter. Then, the average fiber diameters (270 and 1390 nm) differed only because of PHBV concentration because the parameters B, C, and F were identical in this comparison. Thus, the difference 1390 − 270 nm = 1120 nm indicated one measure of the PHBV concentration effect. The other three measures of the PHBV concentration effect were 1675 − 293.5 nm = 1381.5 nm, 1550 − 1590 nm = −40 nm, and 1285 − 975 nm = 310 nm. The main effect of PHBV concentration was defined as the average of these four measures, which was 692.88 nm. Even though parameters D, E, and/or G really influenced the fiber diameter, the estimated main effect was still reliable, which is explained as follows. In the first and the third measures, the differences were calculated by supposing that the parameter D was changed from "+" level to "−" level. However, in the second and the fourth measure, the differences were calculated by supposing that the parameter D was changed from "−" level to "+" level. Therefore, the average value of the four measures would not indicate the effect of parameter D, even though parameter D could really significantly affect the fiber diameter. Similarly, the average value of the four measures would not indicate the effect of parameter E or G. Using the same strategy, the main effects of other parameters were calculated and are shown in Table V. The negative sign means that the change of a certain parameter from low level to high level causes the reduction in fiber diameter or percentage of highly aligned fibers. Although it has been found through the one-factor-at-a-time method that the electrospun PHBV fiber diameter generally increased with PHBV solution concentration and needle inner diameter, this

TABLE III
Factorial Design for Studying the Effects of the Seven Electrospinning Parameters on PHBV Fiber Diameter

Exp No.	a/A	b/B	c/C	ab/D	ac/E	bc/F	abc/G	Fiber diameters from individual runs (nm)		Difference of duplicate (nm)	Estimated variance at each set of conditions, s_i^2 = (Difference)^2/2	Average fiber diameter used in analysis (nm)
1	−	−	−	+	+	+	−	240	300	−60	1,800	270 ± 187
2	+	−	−	−	−	+	+	1,210	1,570	−360	64,800	1,390 ± 187
3	−	+	−	−	+	−	+	340	247	93	4,324.5	293.5 ± 187
4	+	+	−	+	−	−	−	1,580	1,770	−190	18,050	1,675 ± 187
5	−	−	+	+	−	−	+	1,390	1,790	−400	80,000	1,590 ± 187
6	+	−	+	−	+	−	−	1,620	1,480	140	9,800	1,550 ± 187
7	−	+	+	−	−	+	−	980	970	10	50	975 ± 187
8	+	+	+	+	+	+	+	1,060	1,510	−450	101,250	1,285 ± 187
											Total: 280,074.5	

s^2 = pooled estimate of σ^2 = average of estimated variances = $V_{total}/8$ = 35,009.31.
s = 187 nm.

TABLE IV
Factorial Design for Studying the Effects of the Seven Electrospinning Parameters on PHBV Fiber Alignment

Exp No.	a/A	b/B	c/C	ab/D	ac/E	bc/F	abc/G	Percentage of highly aligned fibers[a] (%)		Difference of duplicate (%)	Estimated variance at each set of conditions, s_i^2 = (Difference)^2/2	Percentage used in analysis (%)
1	−	−	−	+	+	+	−	35	48	−13	84.5	41.5 ± 5.04
2	+	−	−	−	−	+	+	99	88	11	60.5	93.5 ± 5.04
3	−	+	−	−	+	−	+	16	15	1	0.5	15.5 ± 5.04
4	+	+	−	+	−	−	−	67	70	−3	4.5	68.5 ± 5.04
5	−	−	+	+	−	−	+	37	32	5	12.5	34.5 ± 5.04
6	+	−	+	−	+	−	−	32	35	−3	4.5	33.5 ± 5.04
7	−	+	+	−	−	+	−	75	83	−8	32	79 ± 5.04
8	+	+	+	+	+	+	+	42	39	3	4.5	40.5 ± 5.04
											Total: 203.5	

s^2 = pooled estimate of σ^2 = average of estimated variances = $V_{total}/8$ = 25.44.
s = 5.04%.
[a] Highly aligned fibers are defined as the fibers that aligned between 80° and 100° relative to the longitudinal axis of the rotating cylinder.

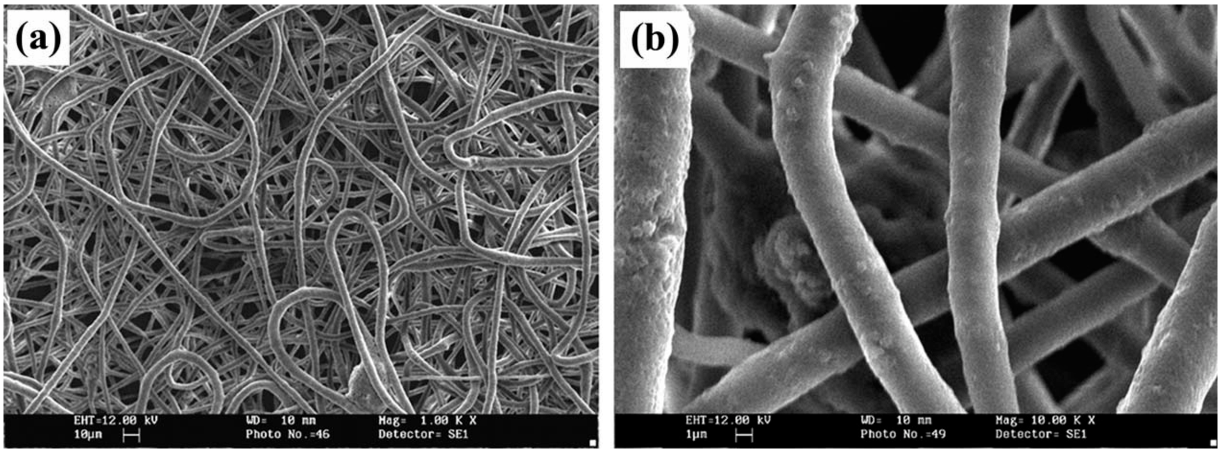

Figure 1 Electrospun fibers with diameters of over 1 μm (from Exp. No. 5): (a) low magnification and (b) high magnification.

approach could not quantify the degree of influence of each parameter.[26] The currently adopted factorial design approach has advantages in that this approach can not only show whether the fiber diameter increases or decreases with one parameter from the sign of the main effect but also indicate the degree of influence of each parameter from the magnitude of the main effect.

Estimation of the standard errors of the effects

According to the pairs of results recorded at the eight different parameter combinations in Table III, an estimate of variance from any individual difference d between duplicated runs was $s^2 = d^2/2$. The average of these estimates yielded a pooled estimate $s^2 = 35{,}009.31$, as shown in Table III. Because each estimated main effect was a difference between two averages of the eight observations, the variance and the standard error (SE) of a main effect on fiber diameter were given as

$$\text{Variance(effect)} = \left(\frac{1}{8}+\frac{1}{8}\right) \times s^2 = \frac{35009.31}{4} = 8752.33 \quad (1)$$

$$\text{SE(effect)} = \sqrt{\text{Variance(effect)}} = 93.55 \quad (2)$$

The variance and the SE of a main effect on fiber alignment were estimated similarly, which were 6.36 and 2.52, respectively. To determine which effects were virtually reliable and which might easily be explained by chance variation, a general guide was used such that effects greater than four times their SE were not readily explained by chance alone. In Table V, effects practically not caused by chance (i.e., effects greater than four times their SE) are marked with a superscript "a."

Further analysis by the 2^3 factorial design

Let the italic of X (i.e., X) be the main effect of parameter X, XY be the interaction effect of parameters

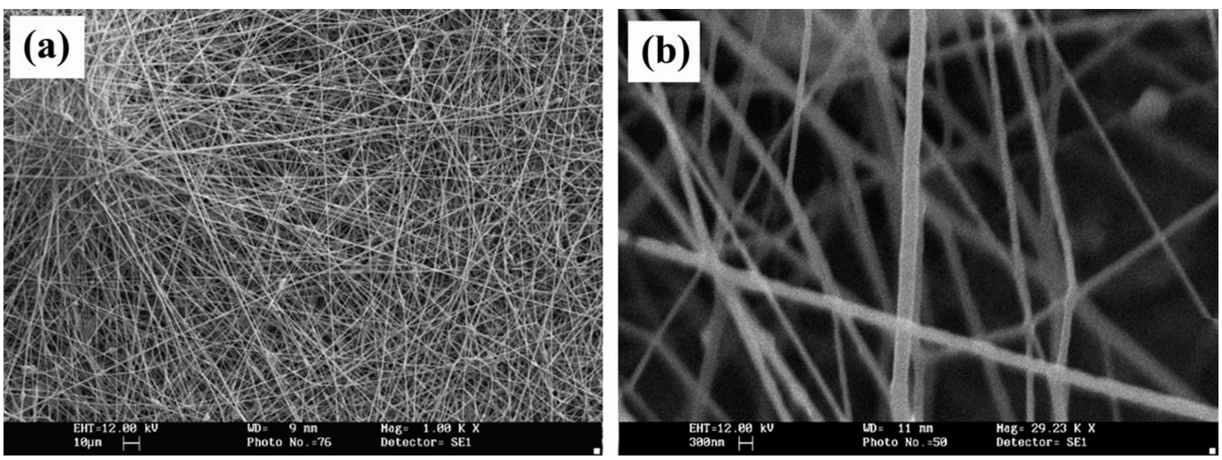

Figure 2 Electrospun fibers with diameters of a few hundred nanometers (from Exp. No. 1): (a) low magnification and (b) high magnification.

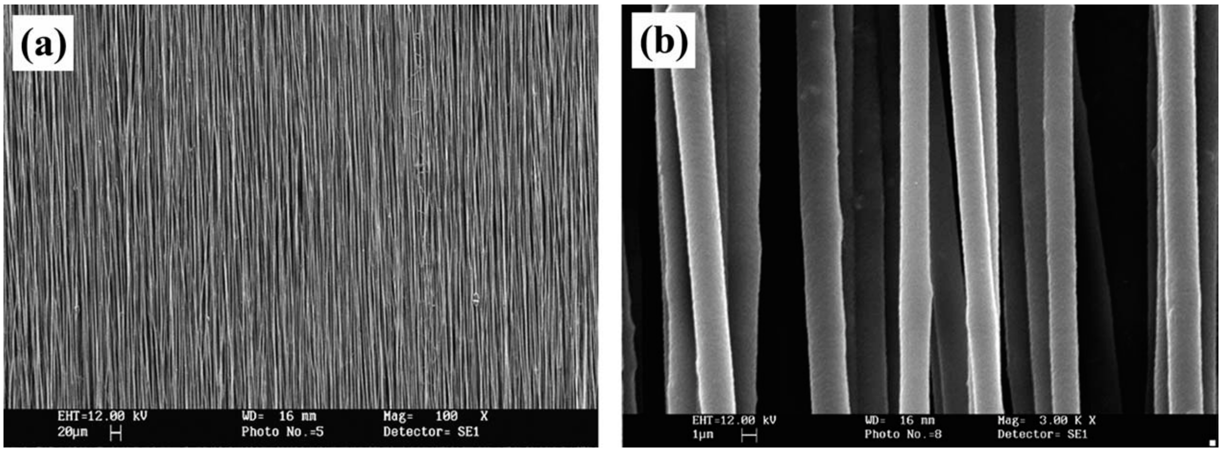

Figure 3 Electrospun aligned fibers (from Exp. No. 2): (a) low magnification and (b) high magnification.

X and Y, and l_X be the contrast actually computed for parameter X. For example, A means the main effect of PHBV concentration, whereas AC means the interaction effect of PHBV concentration and needle inner diameter. l_A denotes the contrast actually computed for PHBV concentration. It was noted that Exp. No. 1 and Exp. No. 3 rendered the results with the smallest average fiber diameters (Table III) and these runs were the only runs in which parameters A, C, and E were changed simultaneously. Therefore, it seemed that either maximum or minimum possible fiber diameters could be achieved if these changes were made, but this statement might not be correct. Table VI lists the estimated effects on fiber diameter with the alias structure. Three of the estimated effects (l_A, l_C, and l_E) were significantly higher than the SE, but the alias structure in Table VI shows that the results allowed four equally reliable but different interpretations. The large effects on fiber diameter could be due to (1) A, C, and E; (2) A, C, and AC; (3) A, E, and AE; or (4) C, E, and CE. To distinguish between the four possible solutions, additional experiments based on the 2^3 factorial design were conducted for the parameters A, C, and E. Figure 5(a) illustrates a cube plot of the Exp. No. for these three parameters. It can be seen that the first eight runs did not produce a complete 2^3 factorial design in the three parameters but only a duplicated half replicate. Therefore, four additional runs (Exp. Nos. 9, 10, 11, and 12) were made at the four missing points in Figure 5(b) and, a combined array, which produced a complete 2^3 factorial design in parameters A, C, and E with four runs replicated, is displayed in Figure 5(c). The results of the combined array are shown in Table VII. All main effects (l_A, l_C, and l_E) could then be estimated by using the method described in the section Estimation of the Main Effects. However, each main effect was just an average of four individual comparisons. This was still an incomplete description of the influence of a certain parameter. For example, it was not known whether the PHBV concentration effect was greater when a larger needle was used, or whether the needle diameter effect was more significant when BTEAC was added. To answer these questions, the interaction effects were estimated. Consider the interaction effect of PHBV concentration and needle inner diameter (AC) on fiber diameter as an example to answer the first aforementioned question. A measure of this interaction was supplied by the difference between the PHBV concentration effects (A) at the plus and minus levels of the needle factor. Let A_+ and A_- be the PHBV concentration effects at the plus and minus levels of the needle factor, respectively.

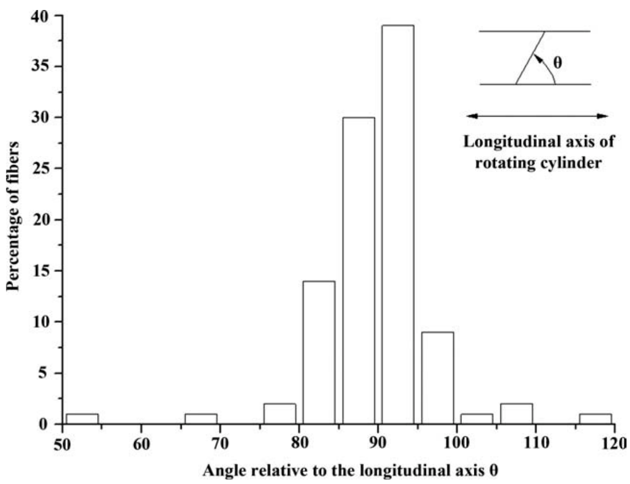

Figure 4 Histogram depicting the degree of fiber alignment of the aligned fibers shown in Figure 3.

$$A_+ = \frac{(1595 - 1282.5) + (1417.5 - 287.5)}{2} = 721.25\ \text{nm} \quad (3)$$

TABLE V
Main Effects of the Seven Electrospinning Parameters on PHBV Fiber Diameter and Alignment

	Electrospinning parameter	Main effect on fiber diameter with standard error (nm)	Main effect on percentage of highly aligned fibers with standard error (%)
A	Concentration of PHBV	692.88 ± 93.55[a]	16.38 ± 2.52[a]
B	Electrospinning voltage	−142.88 ± 93.55	0.13 ± 2.52
C	Needle inner diameter	442.88 ± 93.55[a]	−7.88 ± 2.52
D	Solution feeding rate	152.88 ± 93.55	−9.13 ± 2.52
E	Concentration of BTEAC	−557.88 ± 93.55[a]	−36.13 ± 2.52[a]
F	Rotational speed of fiber collector	−297.13 ± 93.55	25.63 ± 2.52[a]
G	Working distance	22.13 ± 93.55	−9.63 ± 2.52

[a] Effects practically not by chance (i.e., effects greater than four times their standard error).

$$A_{-} = \frac{(1532.5 - 1405) + (704 - 281.75)}{2} = 274.88 \text{ nm} \tag{4}$$

The interaction effect of PHBV concentration and needle inner diameter (*AC*) was given by one-half of this difference, which was 223.19 nm. As this result was less than four times of the SE calculated in Table VII (i.e., 106.45×4 = 425.8 nm), it seemed that the PHBV concentration effect was not significantly depended on needle diameter. The other interaction effects could be estimated similarly. All main effects (*A*, *C*, and *E*) and interaction effects (*AC*, *AE*, and *CE*) with SEs are shown in Table VIII. Again, the effects greater than four times their SE are marked with superscripts. The results shown in Table VIII demonstrated that the parameters behaved independently without interactions in their effects on fiber diameter. Assume that the fiber diameter changed approximately at a constant rate between the two levels of the parameters. All the various conditions of the parameters A, C, and E that give a certain fiber diameter, say 1500 nm, could be found. Referring to the edge of the cube joining Exp. No. 5/7 and 10 in Figure 5(c), the result of 1282.5 nm at the left-hand side of this edge (i.e., Exp. No. 5/7) and the result of 1595 nm at the right-hand side of this edge (i.e., Exp. No. 10) are seen. Therefore, the diameter of 1500 nm should be along this line, nearer to the right-hand side than the left-hand side. This point was marked with a dot in Figure 6(a), according to the calculated proportions. The other points representing the diameter of 1500 nm were marked similarly along the edges joining Exp. No. 10 and 6/8, Exp. No. 12 and 2/4, as well as Exp. No. 2/4 and 11. By joining the dots together, a plane marked 1500 nm was obtained [Fig. 6(a)]. The plane, thus, approximately indicated all the various combinations of the parameters, including PHBV concentration, BTEAC concentration, and needle diameter, which should give a fiber diameter of approximately 1500 nm. A contour plane of 500 nm was plotted similarly in Figure 6(a). The contour planes clearly showed that the fiber diameter increased with increasing PHBV concentration, but significantly reduced with addition of BTEAC. The effects of PHBV concentration and BTEAC addition on PHBV fiber diameter were more significant than that of needle diameter. To prove/disprove the contour planes, five additional fibrous membranes were electrospun with fixed parameters selected from the planes. As shown in Table IX, the actual fiber diameters were very similar to the predicted values from the contour planes. The effects of various parameters

TABLE VI
Estimated Effects on PHBV Fiber Diameter and the Corresponding Alias Patterns for the 2^{7-4}_{III} Factorial Design Experiment

	Electrospinning parameter	Estimated effect	The corresponding alias pattern
A	Concentration of PHBV	$l_A = 692.88$[a]	$A' + BD + CE' + FG$
B	Electrospinning voltage	$l_B = -142.88$	$B + AD + CF + EG$
C	Needle inner diameter	$l_C = 442.88$[a]	$C' + AE' + BF + DG$
D	Solution feeding rate	$l_D = 152.88$	$D + AB + CG + EF$
E	Concentration of BTEAC	$l_E = -557.88$[a]	$E' + AC' + BG + DF$
F	Rotational speed of fiber collector	$l_F = -297.13$	$F + AG + BC + DE$
G	Working distance	$l_G = 22.13$	$G + AF + BE + CD$

[a] Effects practically not by chance (i.e., effects greater than four times their standard error).

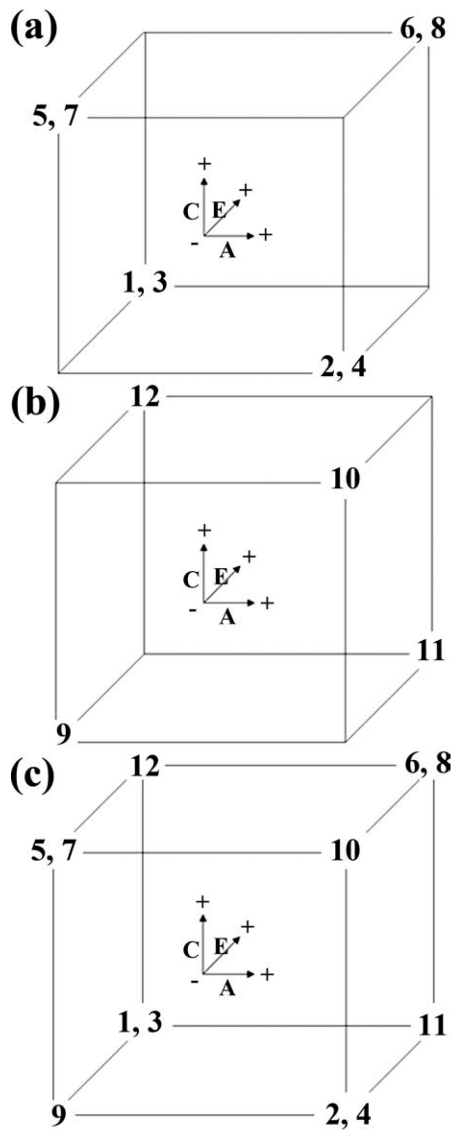

Figure 5 Cube plots of the Exp. No. for parameters A, C, and E: (a) original eight runs, (b) four additional runs, and (c) combined arrays.

on PHBV fiber alignment were investigated similarly, and the corresponding contour planes are illustrated in Figure 6(b). The contour planes, which show the combination of parameters to achieve 30% and 90% of highly aligned fibers, provided a useful summary of how the degree of fiber alignment depended on PHBV concentration, BTEAC concentration, and rotational speed of the fiber-collecting cylinder. In particular, it illustrated that high PHBV concentration and rotational speed facilitated the formation of highly aligned fibers. However, addition of BTEAC might reduce the percentage of highly aligned fibers. Similarly, the contour planes were proved/disproved through additional experiments. As shown in Table X, the actual percentages of highly aligned fibers were very close to the predicted values from the contour planes.

TABLE VII
Factorial Design for Studying the Effects of Parameters A, C, and E on PHBV Fiber Diameter

Exp No.	A	C	E	Fiber diameter from individual runs (nm)		Difference of duplicate (nm)	Estimated variance at each set of conditions, $s_i^2 = (\text{Difference})^2/2$	Average fiber diameter used in analysis (nm)
9	−	−	−	1,330	1,480	−150	11,250	1,405
2, 4	+	−	−	1,390	1,675	−285	40,612.5	1,532.5
5, 7	−	+	−	1,590	975	615	189,112.5	1,282.5
10	+	+	−	1,390	1,800	−410	84,050	1,595
1, 3	−	−	+	270	293.5	−23.5	276.125	281.75
11	+	−	+	680	728	−48	1,152	704
12	−	+	+	265	310	−45	1,012.5	287.5
6, 8	+	+	+	1,550	1,285	265	35,112.5	1,417.5
							Total: 362,578.1	

s^2 = pooled estimate of σ^2 = average of estimated variances = $V_{\text{total}}/8 = 45{,}322.27$.
$s = 212.9$ nm.

$$\text{Variance(effect)} = \left(\frac{1}{8} + \frac{1}{8}\right) \times s^2 = 11330.57$$

$$\text{SE(effect)} = \sqrt{\text{Variance(effect)}} = 106.45$$

TABLE VIII
Main Effects Estimated from Exp. No. 1–12 (Effects on Fiber Diameter ± Standard Error)

Effect due to a single parameter	Interaction effect
$l_A = 498.06 \pm 106.45^a$	$l_{AC} = 223.19 \pm 106.45$
$l_C = 164.81 \pm 106.45$	$l_{AE} = 278.06 \pm 106.45$
$l_E = -781.06 \pm 106.45^a$	$l_{CE} = 194.81 \pm 106.45$

[a] Effects practically not by chance (i.e., effects greater than four times their standard error).

Effects of various parameters

A series of experiments according to the 2^{7-4}_{III} fractional design shows that solution concentration invoked the highest main effect on fiber diameter (693 nm), followed by addition of BTEAC (−558 nm), needle inner diameter (443 nm), rotational speed of the cylinder (−297 nm), solution feeding rate (153 nm), electrospinning voltage (−143 nm), and working distance (22 nm). As the main effects of PHBV concentration, BTEAC concentration and needle inner diameter were four times greater than the SE (94 nm), the main effects of these three parameters could not be easily explained by chance alone. When these three parameters were subjected to the 2^3 factorial design for additional experimental runs, it was found that the effects of solution concentration and BTEAC addition on fiber diameter were significantly higher than that of the needle inner diameter. With increased PHBV concentration, the polymer chain entanglements within the solution became greater. Therefore, it was more difficult for the charges on the polymer jet to stretch the jet into finer fibers. The addition of BTEAC increased the electrical conductivity of the polymer jet, which facilitated the stretching of the jet by the electric force during electrospinning. This caused the reduction in fiber diameter. A needle with a larger orifice diameter might facilitate the formation of a larger Taylor cone during electrospinning, which, in turn,

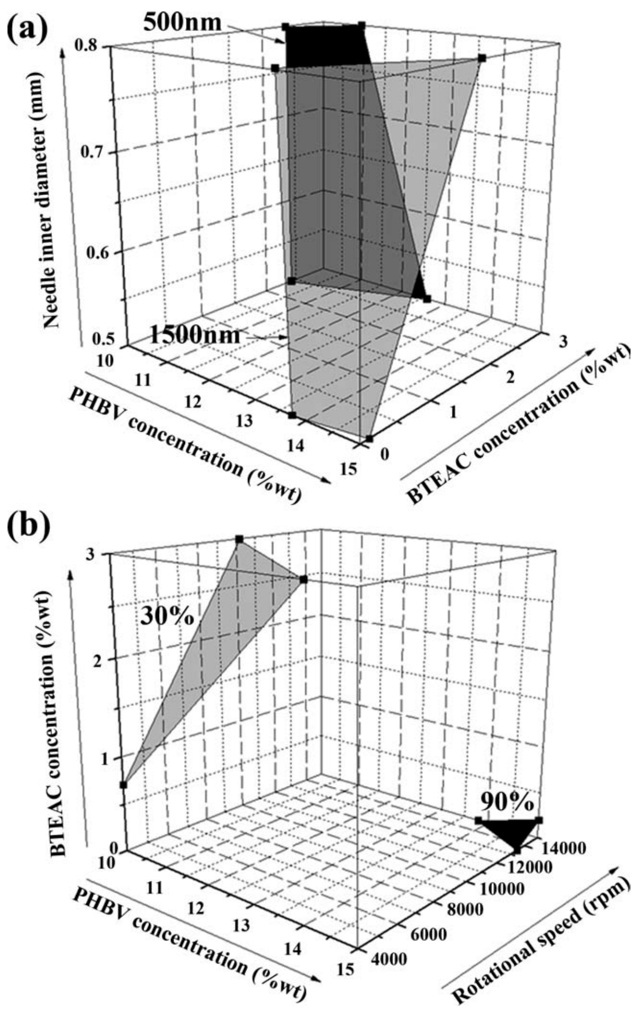

Figure 6 Contour planes illustrating (a) fiber diameter = 500 or 1500 nm and (b) percentage of highly aligned fibers = 30% or 90%.

TABLE IX
Comparison between Experimentally Determined Fiber Diameters and Predicted Fiber Diameters from the Contour Plane

	Fiber diameter (nm)	
Electrospinning parameters	Predicted value	Experimental result
A random set of parameters on the 1500-nm contour plane: PHBV concentration (14.4 wt %); BTEAC concentration (1 wt %); needle inner diameter (0.7 mm)	1500	1578 ± 321
A random set of parameters on the 500-nm contour plane: PHBV concentration (11.6 wt %); BTEAC concentration (2.8 wt %); needle inner diameter (0.6 mm)	500	417 ± 96

TABLE X
Comparison between Experimentally Determined Percentages of Highly Aligned Fibers and Predicted Percentages of Highly Aligned Fibers from the Contour Plane

	Percentage of highly aligned fibers (%)	
Electrospinning parameters	Predicted value	Experimental result
A random set of parameters on the 30% contour plane: PHBV concentration (11.5 wt %); rotational speed of fiber collector (6000 rpm); BTEAC concentration (2 wt %)	30	32 ± 5
A random set of parameters on the 90% contour plane: PHBV concentration (14.8 wt %); rotational speed of fiber collector (13,000 rpm); BTEAC concentration (0.2 wt %)	90	86 ± 8

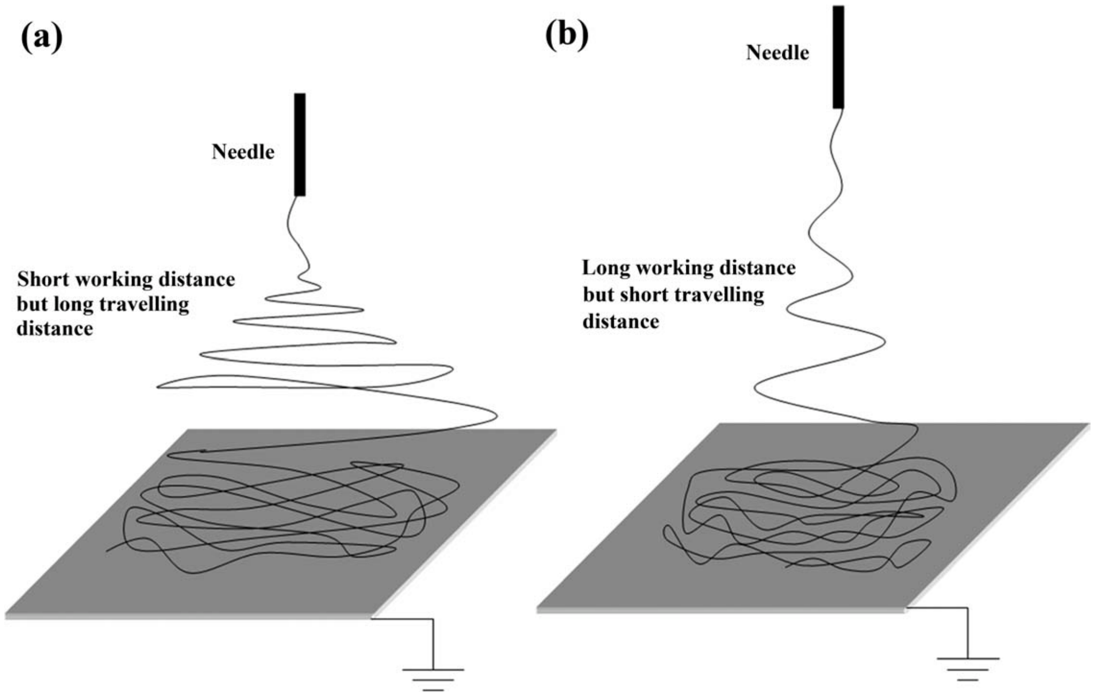

Figure 7 Schematic diagrams showing different trajectories of electrospun polymer jets at different working distances.

facilitates the ejection of a larger initial jet and, hence, a larger diameter fiber. Although the effect of rotational speed of the cylinder on fiber diameter was not as significant as that of the parameters such as PHBV concentration and BTEAC concentration, the effect was still much greater than that of solution feeding rate, electrospinning voltage, or working distance. This shows that the fibers might be stretched into thinner fibers when they landed on the surface of the rotating cylinder. Higher rotational speed enhanced the stretching ability and, thus, resulted in thinner fibers. Higher solution feeding rate could just push more solution to the needle tip within the same period of time. The size of the Taylor cone or the initiating jet would not be significantly affected by the varying the solution feeding rate. Therefore, the effect of solution feeding rate on fiber diameter was not so significant. Higher voltage might affect the polymer jet in two different ways simultaneously during electrospinning. On one hand, this induced a larger initiating jet and, hence, facilitated the formation of larger-diameter fibers. On the other hand, this allowed a more effective stretching of the jet by electric forces, which facilitated the formation of thinner fibers. These two effects might cancel each other during electrospinning; thus, the fiber diameter was not markedly influenced by varying the electrospinning voltage. Working distance was still not an effective parameter for controlling the fiber diameter because of the inconsistency of trajectory of the polymer jet. Ideally, a longer working distance should render a longer traveling distance of the jet, which, in turn, provides more time for the jet to be stretched before landing on the collector, and, hence, the fiber diameter should be smaller. However, the traveling distance of the jet might not be proportional to the working distance because of the complicated three-dimensional spiraling trajectory of the jet. Figure 7(a) shows a long traveling distance at a short working distance, whereas Figure 7(b) shows a short traveling distance at a long working distance. With these situations, the fibers obtained in Figure 7(a) should exhibit smaller diameters, even though the working distance is shorter. Therefore, varying the working distance may not be a reliable way to control the fiber diameter.

The contour planes in Figure 6(b) illustrates with great clarity that the degree of fiber alignment was improved by increasing rotational speed of the cylinder and PHBV concentration, or reducing the amount of BTEAC. If the rotational speed was faster than the traveling speed of the jet at the point of fiber collection, the solidified jet would be quickly winded by the cylinder and became an aligned fiber. If the collector speed was slower than the jet speed (traveling speed), the jet would be deposited on the cylinder surface in any direction and will become a randomly oriented fiber. During electrospinning, the polymer jet exhibited different traveling speeds, which depended on the electrical force and the mass of the jet. Figure 8(a) shows an approximate distribution of the percentage of fibers against the traveling speeds of the jet at the point of fiber collection (i.e., landing speed). Obviously, a higher collector

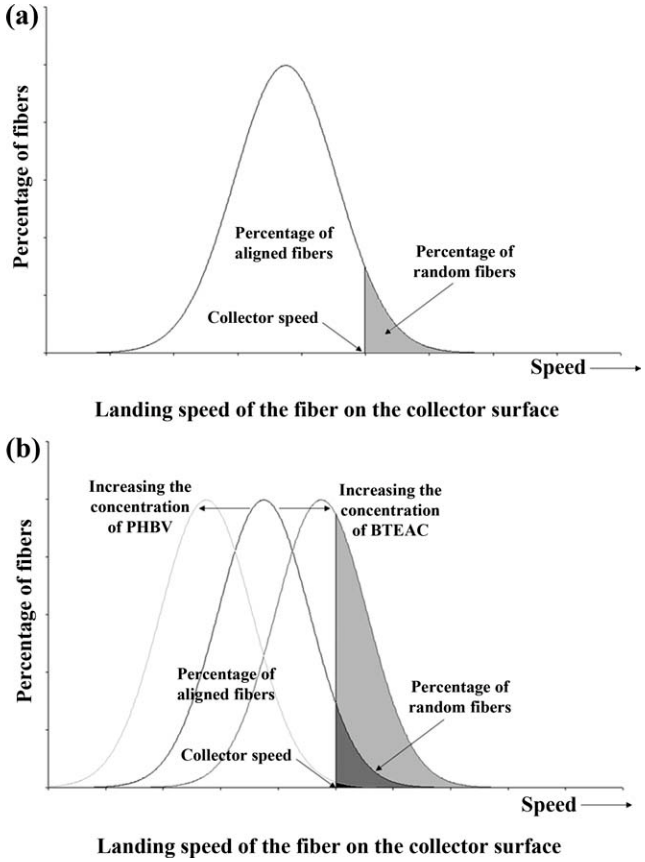

Figure 8 Approximate distributions of the percentage of fibers at different landing speeds: (a) effect of collector rotational speed on percentage of aligned fibers and (b) effects of PHBV concentration and BTEAC concentration on percentage of aligned fibers.

speed allows a larger proportion of fibers to be collected in a highly aligned manner. When the concentration of PHBV became higher, the mass of the jet would be increased, which shifted the traveling speed profile to a low-speed region [Fig. 8(b)]. On the contrary, addition of BTEAC increased the conductivity of the jet, and, hence, the electrical force, which shifted the traveling speed profile to a high-speed region [Fig. 8(b)]. Therefore, a higher PHBV concentration (lower jet landing speed) improved the degree of fiber alignment, whereas a higher BTEAC concentration (higher jet landing speed) facilitated the formation of random fibers, provided that the collector rotational speed was unchanged.

In this study of finding the boundary values, it was found that the electrospun PHBV fiber diameter increased monotonically with increasing PHBV solution concentration and needle inner diameter when these parameters were varied between the boundary values shown in Table II. A monotonic increase in electrospun fiber diameter with increasing solution concentration[13,37] and increasing needle inner diameter[18] were also reported when different polymers were used. It was shown in this study that the percentage of highly aligned PHBV fibers increased monotonically with increasing rotational speed of the fiber collector and PHBV solution concentration but decreasing BTEAC concentration when these parameters were varied between the boundary values shown in Table II. All these findings suggested that the intermediate values between the two boundaries should have similar influence with the boundary values.

Despite the success in controlling the PHBV fiber diameter and fiber alignment with the help of careful analysis *via* the factorial design approach, it should be noted that the optimized parameters for electrospinning PHBV reported in this study may not be extrapolated to all polymers because different polymers have different molecular weights and the corresponding polymer solutions have different conductivity and surface tension. However, the approach adopted in this study can be used for many, if not all, polymers for electrospinning desirable fibrous structures.

CONCLUSIONS

This study has clearly demonstrated that PHBV can be electrospun into microfibers and nanofibers in either highly aligned or randomly oriented manner. Polymer solution concentration and conductivity-enhancing salt content are the major influencing factors on electrospun fiber diameter. Their increases cause increase and decrease, respectively, of the fiber diameter. The degree of fiber alignment can be improved by using high polymer solution concentration and high rotational speed of the fiber collector but small amount of conductivity-enhancing salt. Other parameters such as electrospinning voltage, solution feeding rate, and working distance are relatively less influential in affecting the fiber diameter and alignment. Successful control of fiber diameter and alignment during electrospinning is important for constructing desirable fibrous scaffolds for various tissue engineering applications.

The authors acknowledge the assistance provided by technical staff in the Department of Mechanical Engineering, HKU.

References

1. Kumbar, S. G.; James, R.; Nukavarapu, S. P.; Laurencin, C. T. Biomed Mater 2008, 3, 034002.
2. Sill, T. J.; von Recum, H. A. Biomaterials 2008, 29, 1989.
3. Nisbet, D. R.; Forsythe, J. S.; Shen, W.; Finkelstein, D. I.; Horne, M. K. J Biomater Appl 2009, 24, 7.
4. Agarwal, S.; Wendorff, J. H.; Greiner, A. Adv Mater 2009, 21, 3343.

5. Ayres, C. E.; Jha, B. S.; Sell, S. A.; Bowlin, G. L.; Simpson, D. G. Wiley Interdiscipl Rev Nanomed Nanobiotechnol 2010, 2, 20.
6. Vaz, C. M.; van Tuijl, S.; Bouten, C. V. C.; Baaijens, F. P. T. Acta Biomater 2005, 1, 575.
7. Stevens, M. M.; George, J. H. Science 2005, 310, 1135.
8. Lee, J. H.; Rim, N. G.; Jung, H. S.; Shin, H. Macromol Biosci 2010, 10, 173.
9. Tong, H. W.; Wang, M. J Nanosci Nanotechnol 2007, 7, 3834.
10. Yang, X.; Yang, F.; Walboomers, X. F.; Bian, Z.; Fan, M.; Jansen, J. A. J Biomed Mater Res A 2010, 93, 247.
11. Sanders, J. E.; Cassisi, D. V.; Neumann, T.; Golledge, S. L.; Zachariah, S. G.; Ratner, B. D.; Bale, S. D. J Biomed Mater Res A 2003, 65, 462.
12. Chen, M.; Patra, P. K.; Warner, S. B.; Bhowmick, S. Tissue Eng 2007, 13, 579.
13. Badami, A. S.; Kreke, M. R.; Thompson, M. S.; Riffle, J. S.; Goldstein, A. S. Biomaterials 2006, 27, 596.
14. Moroni, L.; Licht, R.; De Boer, J.; De Wijn, J. R.; Van Blitterswijk, C. A. Biomaterials 2006, 27, 4911.
15. Baker, S. C.; Atkin, N.; Gunning, P. A.; Granville, N.; Wilson, K.; Wilson, D.; Southgate, J. Biomaterials 2006, 27, 3136.
16. Buchko, C. J.; Chen, L. C.; Shen, Y.; Martin, D. C. Polymer 1999, 40, 7397.
17. Cui, W.; Li, X.; Zhou, S.; Weng, J. J Appl Polym Sci 2007, 103, 3105.
18. Katti, D. S.; Robinson, K. W.; Frank, K. K.; Cato, T. L. J Biomed Mater Res B 2004, 70, 286.
19. Kidoaki, S.; Kwon, I. K.; Matsuda, T. Biomaterials 2005, 26, 37.
20. Li, Q.; Yang, Y.; Jia, Z.; Guan, Z. High Volt Eng 2007, 33, 186.
21. Lyons, J.; Li, C.; Ko, F. Polymer 2004, 45, 7597.
22. Mo, X. M.; Xu, C. Y.; Kotaki, M.; Ramakrishna, S. Biomaterials 2004, 25, 1883.
23. Sukigara, S.; Gandhi, M.; Ayutsede, J.; Micklus, M.; Ko, F. Polymer 2003, 44, 5721.
24. Sukigara, S.; Gandhi, M.; Ayutsede, J.; Micklus, M.; Ko, F. Polymer 2004, 45, 3701.
25. Tan, S. H.; Inai, R.; Kotaki, M.; Ramakrishna, S. Polymer 2005, 46, 6128.
26. Tong, H. W.; Wang, M.;Key Eng Mat 2007, 334–335, 1233.
27. Yordem, O. S.; Papila, M.; Menceloglu, Y. Z. Mater Design 2008, 29, 34.
28. Chew, S. Y.; Mi, R.; Hoke, A.; Leong, K. W. Biomaterials 2008, 29, 653.
29. Mills, C. A.; Fernandez, J. G.; Martinez, E.; Funes, M.; Engel, E.; Errachid, A.; Planell, J.; Samitier, J. Small 2007, 3, 871.
30. Xu, C. Y.; Inai, R.; Kotaki, M.; Ramakrishna, S. Biomaterials 2004, 25, 877.
31. Yang, F.; Murugan, R.; Wang, S.; Ramakrishna, S. Biomaterials 2005, 26, 2603.
32. Box, G. E. P.; Hunter, J. S.; Hunter, W. G. Statistics for Experimenters; John Wiley & Sons, Inc.: Hoboken, NJ, 2005.
33. Wang, C.; Hsu, C. H.; Hwang, I. H. Polymer 2008, 49, 4188.
34. Kwon, O. H.; Lee, I. S.; Ko, Y. G.; Meng, W.; Jung, K. H.; Kang, I. K.; Ito, Y. Biomed Mater 2007, 2, 52.
35. Meng, W.; Kim, S. Y.; Yuan, J.; Kim, J. C.; Kwon, O. H.; Kawazoe, N.; Chen, G.; Ito, Y.; Kang, I. K. J Biomater Sci Polym Ed 2007, 18, 81.
36. Chan, K. H. K.; Wong, S. Y.; Li, X.; Zhang, Y. Z.; Lim, P. C.; Lim, C. T.; Kotaki, M.; He, C. B. J Phys Chem B 2009, 113, 13179.
37. Chieh, C.; Kevin, L.; Liwei, L. Appl Phys Lett 2008, 93, 123111.